MECHANICAL

TECHNOLOGY

INCORPORATED

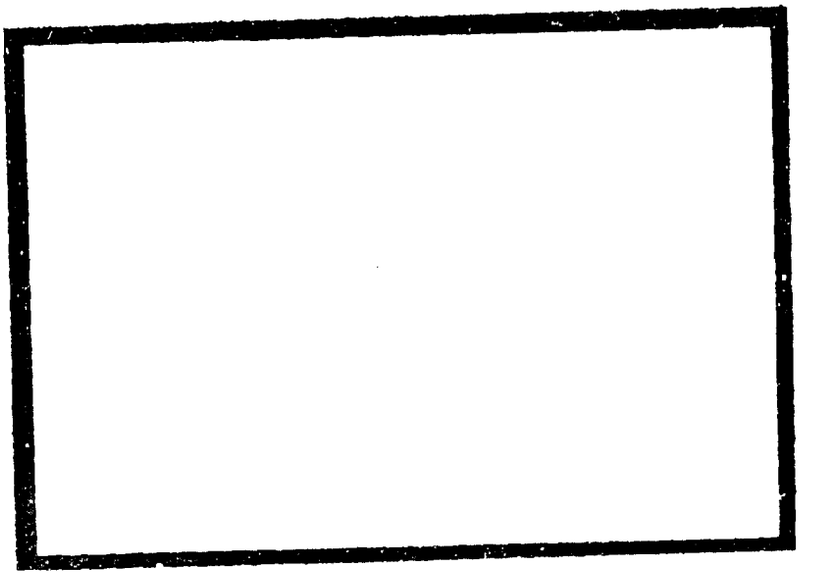

MECHANICAL TECHNOLOGY INCORPORATED
968 Albany-Shaker Road
Latham, New York 12110

MTI-66TR47

ANALYSIS OF PNEUMATIC HAMMER INSTABILITY OF INHERENTLY COMPENSATED HYDROSTATIC THRUST GAS BEARINGS

by

T. Chiang
C.H.T. Pan

Contract Nonr-3730(00)
Task No. NR 062-317/4-7-66

NO. MTI-661R47

DATE: January, 1967

TECHNICAL REPORT

ANALYSIS OF PNEUMATIC HAMMER INSTABILITY OF INHERENTLY COMPENSATED HYDROSTATIC THRUST GAS BEARINGS

by

T. Chiang
C.H.T. Pan

T. Chiang C. H. T. Pan

Author (s)

E. B Arwas

Approved

Approved

Prepared under

Contract No. Nonr-3730(00)
Task No. NR 062-317/4-7-66

Prepared for

Office of Naval Research
Department of the Navy

Administered by

Office of Naval Research
Department of the Navy

MTI
MECHANICAL TECHNOLOGY INCORPORATED

968 ALBANY - SHAKER ROAD — LATHAM, NEW YORK — PHONE 785-0922

TABLE OF CONTENTS

ABSTRACT

Pneumatic hammer instability of an inherently compensated thrust gas bearing was analyzed theoretically. Vohr's experimental correlation between the pressure loss coefficient and Reynold's number was used to calculate flow through the restrictor instead of using the nozzle equations. The time dependent Reynold's equation was solved by a perturbation analysis for small axial oscillation. Based on the perturbation analysis, dynamic stiffness and damping coefficient were calculated. Utilizing these and Pan's stability criteria (Ref. 6) stability maps were constructed.

1. INTRODUCTION

Externally pressurized gas bearings have been used in many engineering devices. It is well known that in order for the bearing to have relatively large load capacity and stiffness it is desirable to have recessed pockets immediately after the feeding holes. This causes the externally pressurized gas bearings to be susceptible to pneumatic hammer instability. Analytical investigations on this subject were made in References 1, 2 and 3.

In conventional analyses of externally pressurized bearings, nozzle equations are used in calculating the flow across a restrictor. The dynamic pressure head resulting from expansion through the restrictor is assumed to be completely lost when entering the bearing film. This, however, is not true as reported in References 4 and 5; a measurement of pressure at the restrictor exit indicates that there is considerable pressure recovery. It was shown that the pressure loss coefficient can be correlated with the Reynolds' number (Ref. 4); a linear relationship is chosen for simplicity.

A simple thrust plate with a feeding hope at the center and a recessed pocket is to be analyzed based on the above pressure loss coefficient correlation for the restrictor flow and the Reynolds' equation for the bearing film. Perturbation analysis for small oscillation about the equilibrium position will be performed. Based on the perturbation analysis, dynamic bearing stiffness and damping coefficient are calculated. Using the stability analysis of Ref. 6, stability maps are constructed.

2. ANALYSIS - SMALL PERTURBATION

The configuration of an inherently compensated, hydrostatic, circular, thrust bearing is schematically shown in Figure 1. Gas at supply pressure p_s is led through the feeding hole with diameter d_f, into the recessed pocket before entering the bearing film. For a circular bearing it is convenient to use the polar coordinates. If we further assume circular symmetry, i.e. no misalignment, then the radial coordinate, r, is the only space variable required to describe the flow and the pressure distribution. In order to facilitate a dynamic analysis let us allow the bearing to have small axial vibrations about its equilibrium position and express the bearing film thickness as

$$h = C + \varepsilon \cos \tau \tag{2.1}$$

or in dimensionless form

$$\bar{h} = 1 + \bar{\varepsilon} \cos \tau \tag{2.2}$$

where

$$\left.\begin{aligned} \bar{h} &= h/C \\ \bar{\varepsilon} &= \varepsilon/C \\ C &= \text{equilibrium film thickness} \\ \tau &= \omega t = \text{dimensionless time} \\ \omega &= \text{frequency of vibration} \end{aligned}\right] \tag{2.3}$$

We have assumed that the vibrations are purely sinusoidal. Note that $\bar{\varepsilon}$, the normalized amplitude of vibration, is a small number.

The well-known time-dependent, isothermal Reynolds' equation is, in dimensionless form,

$$\frac{1}{\bar{r}} \frac{\partial}{\partial \bar{r}} \left[\bar{r}\, \bar{h}^3\, \bar{p}\, \frac{\partial \bar{p}}{\partial \bar{r}} \right] = \sigma \frac{\partial}{\partial \tau} (\bar{p}\, \bar{h}) \tag{2.4}$$

where

$$\left.\begin{aligned} \bar{r} &= r/R \\ \bar{p} &= p/p_a \\ \sigma &= \frac{12\mu\omega}{p_a} \left(\frac{R}{C}\right)^2 = \text{squeeze number} \end{aligned}\right] \tag{2.5}$$

The boundary conditions are

$$\begin{aligned} &\text{at } \bar{r} = 1 \qquad \bar{p} = 1 \\ &\text{at } \bar{r} = \frac{d_R}{2R}\,, \quad \bar{p} = p_R/p_a = \bar{p}_R \end{aligned} \tag{2.6}$$

While Eq. (2.4) governs the pressure distribution in the bearing film, additional pressure-flow relationships across the inlet restrictions at $\bar{r} = \bar{r}_F$ and at $\bar{r} = \bar{r}_R$ are required for the solution of the problem. In the literature (Ref. 1,2,3) the well-known nozzle formula is used to calculate the expansion of air from p_s to p_F and from p_F to p_R (assume that the pressure is uniform in the recessed pocket; see Appendix A). If the pressures calculated according to the nozzle formula are accepted, one automatically assumes that the velocity head resulting from expansion through the nozzles is completely lost. This is not so because part of the velocity head is recovered as indicated by references 4 and 5. In fact, if we express the pressure drop at the entrance in terms of the velocity head,

$$(\Delta p)_{ent} = K' \frac{\rho V^2}{2} \tag{2.7}$$

where

$$\left.\begin{aligned} &K' = \text{loss coefficient} \\ &\rho = \text{downstream gas density} \\ &V = \text{downstream average velocity} \end{aligned}\right] \tag{2.8}$$

In Ref. 4, K' is correlated experimentally with the Reynolds' number (Re) which is reproduced in Figure 2. But for all practical purposes, a linear relationship between K' and Re is satisfactory,

$$K' = K\,Re = K \frac{\rho V L}{\mu} \tag{2.9}$$

where

$$\left.\begin{aligned} &K = \text{constant} = 0.66 \times 10^{-3} \\ &L = \text{typical length} = \text{film thickness} \end{aligned}\right] \tag{2.10}$$

Thus

$$(\Delta p)_{ent} = K \frac{\rho^2 V^3 L}{2\mu} \tag{2.11}$$

Applying the above equation to the inlet of the recessed pocket we have

$$p_s - p_F = K \frac{\rho_F^2 V_F^3 (h + h_R)}{2\mu} \tag{2.12}$$

Inside the recessed pocket we can write another Reynolds' equation applicable there and solve for the pressure distribution. However, past experience indicates that the gradient of the square of the pressure varies inversely as the cubic of the local film thickness (see Eq. (A-5). In most applications, the depth of the recessed pocket h_R is greater than or at least equal to h. Therefore, it is a good approximation to assume that the pressure in the pocket is uniform so long as d_F/d_R is not too small.

Now, we again apply Equation (2.11) to the inlet to the bearing film (see Figure 1)

$$p_F - p_R = K \frac{\rho_R^2 V_R^3 h}{2\mu} \tag{2.13}$$

In solving the Reynolds' equation (2.4) with small periodic variations of the gap about the equilibrium position, we write in complex form,

$$\bar{h} = 1 + \bar{\varepsilon} e^{i\tau} \tag{2.14}$$

and expand the dimensionless pressure,

$$\bar{p} = \bar{p}_o + \bar{\varepsilon} \bar{p}_1 e^{i\tau} \tag{2.15}$$

taking, of course, only the real part to be of physical significance. To the first order in ε we can compute easily,

$$\left.\begin{aligned} \bar{p}^2 &= \bar{p}_o^2 + 2\bar{\varepsilon} \bar{p}_o \bar{p}_1 e^{i\tau} \\ \bar{p}\bar{h} &= \bar{p}_o + \bar{\varepsilon} (\bar{p}_o + \bar{p}_1) e^{i\tau} \\ \bar{h}^3 &= 1 + 3\bar{\varepsilon} e^{i\tau} \end{aligned}\right\} \tag{2.16}$$

Substitution of the above equations into (2.4) yields the steady-state and perturbation equations,

$$\frac{1}{\bar{r}} \frac{\partial}{\partial \bar{r}} \left[\bar{r} \frac{\partial \bar{p}_o^2}{\partial \bar{r}} \right] = 0 \tag{2.17}$$

$$\frac{1}{\bar{r}} \frac{\partial}{\partial \bar{r}} \left[\bar{r} \frac{\partial}{\partial \bar{r}} (\bar{p}_o \bar{p}_1) \right] = i \sigma (\bar{p}_o + \bar{p}_1) \tag{2.18}$$

The boundary conditions are:

$$\text{at } \bar{r} = 1, \qquad \bar{p}_o = 1, \qquad \bar{p}_1 = 0 \tag{2.19}$$

$$\text{at } \bar{r} = \bar{r}_R = \frac{d_R}{2R}, \qquad \bar{p}_o = \bar{p}_{RO} \tag{2.20}$$

It is to be noted that $\bar{p}_{RO}$ is an unknown quantity to be determined. Furthermore, one additional boundary condition, $\bar{p}_1$ at $\bar{r}_R$ is required to solve the problem. Now we can obtain the steady-state solution of (2.17) in terms of $\bar{p}_{RO}$. Thus,

$$\bar{p}_o = \left[1 + \frac{\bar{p}_{RO}^2 - 1}{\ell n \, \bar{r}_R} \ell n \, \bar{r} \right]^{\frac{1}{2}} \tag{2.1}$$

The radial velocity in the film is, from the Stoke's equation,

$$u = \frac{1}{2\mu} \frac{\partial p}{\partial r} \left(z^2 - \frac{h^2}{4} \right) \tag{2.22}$$

Here z is the axial coordinate (normal to the film) measured from the center of the film; the bearing surfaces are at $z = \pm h/2$ respectively. Knowing the radial velocity distribution across the film, we can calculate the mass flow rate per unit circumferential length at the film inlet,

$$G_R = \int_{-h/2}^{h/2} \rho_R \, u \, dz = \frac{p_R}{RT} \frac{1}{2\mu} \frac{\partial p}{\partial r} \Bigg|_{r_R} \int_{-h/2}^{h/2} \left(z^2 - \frac{h^2}{4} \right) dz$$

$$= \frac{-h^3}{24\mu RT} \frac{\partial p^2}{\partial r} \Bigg|_{r_R} \tag{2.23}$$

Define a mean velocity V_R at the film inlet,

$$G_R = \rho_R V_R h = \frac{p_R}{RT} V_R h \tag{2.24}$$

Equating (2.23) and (2.24) results in

$$p_R V_R = - \frac{h^2}{24\mu} \frac{\partial p^2}{\partial r} \Bigg|_{r_R} = - \frac{h^2}{24\mu} \frac{p_a^2}{R} \frac{\partial \bar{p}^2}{\partial \bar{r}} \Bigg|_{\bar{r}_R} \tag{2.25}$$

Recognizing that

$$\bar{p}_R = \bar{p}_{RO} + \varepsilon\, \bar{p}_{R1}\, e^{i\tau}$$

and

$$\left.\frac{\partial \bar{p}^2}{\partial \bar{r}}\right|_{\bar{r}_R} = \left.\frac{\partial \bar{p}_o^{\,2}}{\partial \bar{r}}\right|_{\bar{r}_R} + 2\varepsilon\, e^{i\tau} \left.\frac{\partial (\bar{p}_o\, \bar{p}_1)}{\partial r}\right|_{\bar{r}_R}$$

Equation (2.25) becomes

$$V_R = -\frac{C^2 p_a}{24\mu R} \frac{1}{E\, \bar{p}_{RO}} \left\{1 + \varepsilon e^{i\tau}\left[2 - \frac{\bar{p}_{R1}}{\bar{p}_{RO}} + 2E \left.\frac{\partial (\bar{p}_o\, \bar{p}\,)}{\partial r}\right|_{r_R}\right]\right\} \tag{2.26}$$

where

$$E = \left[\left.\frac{\partial \bar{p}_o^{\,2}}{\partial \bar{r}}\right|_{\bar{r}_R}\right]^{-1} \tag{2.27}$$

Now that we have an expression for V_R, let us apply the law of mass conservation to the recessed pocket,

$$\frac{\partial}{\partial t}\left[\rho_R V_R r_R h - \rho_F V_F r_F (h + h_R)\right] + \frac{\partial}{\partial t}\left[\rho_F \pi (r_R^2 - r_F^2)(h - h_R)\right] = 0 \tag{2.28}$$

We have assumed that the pressure and hence the density in the recessed pocket be uniform even under dynamic condition. This requires that $\tilde{\sigma} \ll 1$, as shown in Appendix A.

After some algebraic manipulation, Equation (2.28) is reduced to

$$V_F = -\frac{C^2 p_a}{24\mu R} \frac{r_R}{r_F} \frac{1}{\bar{p}_{FO}\,(1 + \bar{h}_R)\,E} \left\{1 + \varepsilon\, e^{i\tau}\left[2 + 2E \left.\frac{\partial (\bar{p}_o\, \bar{p}_1)}{\partial \bar{r}}\right|_{\bar{r}_R} - \frac{\bar{p}_{F1}}{\bar{p}_{FO}} + \frac{\bar{h}_R}{1 + \bar{h}_R} - i\sigma \frac{\bar{r}_R^{\,2} - \bar{r}_F^{\,2}}{\bar{r}_R}\left(\bar{p}_{bo} + (1 + \bar{h}_R)\,\bar{p}_{bi}\right) E\right]\right\} \tag{2.29}$$

We have used Equation (2.26) and the obvious relation

$$\bar{p}_F = \bar{p}_{FO} + \varepsilon\, \bar{p}_{F1}\, e^{i\tau} \tag{2.30}$$

Knowing V_R and V_F from Eq.'s (2.26) and (2.29) respectively, we are now in a position to utilize Eq.'s (2.12) and (2.13). Substituting (2.26) into Eq. (2.13) and collecting terms of the same power of ε, we obtain

$$\bar{P}_{FO} - \bar{P}_{RO} = - K Q_1 \frac{1}{\bar{P}_{RO}} E^{-3} \tag{2.31}$$

$$\bar{P}_{F1} - \bar{P}_{R1} = (\bar{P}_{FO} - \bar{P}_{RO}) \left\{ 7 - 6 \frac{\bar{P}_{R1}}{\bar{P}_{RO}} + 6E \frac{(\bar{P}_o \bar{P}_1)}{\partial \bar{r}} \bigg|_{\bar{r}_R} \right\} \tag{2.32}$$

Similarly, from (2.12) and (2.29),

$$\bar{P}_s - \bar{P}_{FO} = - K Q_1 \frac{1}{\bar{P}_{FO}} E^{-3} \tag{2.33}$$

$$- \bar{P}_{F1} = (\bar{P}_s - \bar{P}_{FO}) \left\{ 6 + \frac{1 + 3\bar{h}_R}{1 + \bar{h}_R} + 6E \frac{\partial(\bar{P}_o \bar{P}_1)}{\partial \bar{r}} \bigg|_{\bar{r}_R} - \frac{\bar{P}_{F1}}{\bar{P}_{FO}} - 3 i \sigma \frac{\bar{r}_R^2 - \bar{r}_F^2}{\bar{r}_R} \left[\bar{P}_{FO} + (1 + \bar{h}_R) \bar{P}_{f1} \right] E \right\} \tag{2.34}$$

where

$$Q_1 = \frac{C^7 p_a^4}{2 \times 24^3 \mu^4 (RT)^2 R^3} \tag{2.35}$$

$$\Gamma = \left(\frac{\bar{r}_R}{\bar{r}_F} \right)^3 (1 + \bar{h}_R)^{-2} = \text{geometry parameter} \tag{2.36}$$

Steady-State Solution

Combining (2.21) and (2.27) results in

$$E = \frac{\bar{r}_R \ln \bar{r}_R}{\bar{P}_{RO}^2 - 1}$$

Thus, we rewrite (2.31) and (2.33) in the form

$$\bar{P}_{RO} (\bar{P}_{FO} - \bar{P}_{RO}) - \frac{1}{\Lambda_1^3 \bar{P}_s^4 \Gamma} (\bar{P}_{RO}^2 - 1)^3 = 0 \tag{2.37}$$

$$\bar{p}_{FO}\,(\bar{p}_s - \bar{p}_{FO}) - \frac{1}{\Lambda_i^3\,\bar{p}_s^4}\,(\bar{p}_{RO}^2 - 1)^3 = 0 \qquad (2.38)$$

where

$$\Lambda_i = \text{modified feeding parameter} = \frac{12\,\mu\sqrt{RT}\,r_F\,(C + h_R)(-\ln \bar{r}_R)}{C^3 p_s}\left[\frac{16\,\mu\sqrt{RT}}{K p_s\,(C + h_R)}\right]^{1/3} \qquad (2.39)$$

Thus, it is revealed from the analysis that an inherently compensated hydrostatic thrust gas bearing has two controlling parameters, namely, a geometry parameter, Γ, and a modified feeding parameter, Λ_i, which is defined in (2.39). The modification is through the factor $\left[\frac{16\,\mu\sqrt{RT}}{K\,p_s\,(C + h_R)}\right]^{1/3}$ as a result of using Vohr's experimental correlation. From the input data for a given configuration, Λ_i and Γ can be calculated. Then, Equations (2.37) and (2.38) are to be solved for $\bar{p}_{FO}$ and $\bar{p}_{RO}$. Since the equations are non-linear, the computations using Newton-Raphson method (Ref. 9) are programmed on a computer. Having solved $\bar{p}_{FO}$ and $\bar{p}_{RO}$, we know the steady-state pressure in the pocket ($\bar{p}_{FO}$), and the pressure distribution in the film is given by Eq. (2.21).

From previous experience (see, for example, References 1 and 2), we know that, in order for a bearing to be stable and to have relatively large load capacity and stiffness, the recessed pocket should have a relatively small volume but large area ($\pi\bar{r}_R^2$). Thus, a shallow pocket ($h_R \gtrsim C$) is desirable. Under these conditions, it is found that Γ is of the order of 1000 or larger. From Equation (2.37), it is seen that when Γ is large (say, 100 or larger), $\bar{p}_{FO} \approx \bar{p}_{RO}$, i.e., the loss at the entrance to the bearing is negligibly small. Therefore, as long as Γ is large, the solution will be insensitive to Γ.

Perturbation Solution

The perturbation pressure is governed by Eq. (2.18) with the boundary condition that $\bar{p}_1 = 0$ at $\bar{r} = 1$. Equations (2.32) and (2.34) are to be used to derive one additional boundary condition required to solve the problem.

Since $\bar{p}_1$ may be complex, it is convenient to assume that

$$\bar{p}_o \, \bar{p}_1 = u + iv \tag{2.40}$$

Substitute into Eq. (18) and separate the real and imaginary parts

$$\frac{1}{\bar{r}} \frac{d}{d\bar{r}} \left[\bar{r} \frac{du}{d\bar{r}} \right] + \frac{\sigma}{\bar{p}_o} v = 0 \tag{2.41}$$

$$\frac{1}{\bar{r}} \frac{d}{d\bar{r}} \left[\bar{r} \frac{dv}{d\bar{r}} \right] - \frac{\sigma}{\bar{p}_o} u = \sigma \bar{p}_o \tag{2.42}$$

with boundary conditions

$$\left.\begin{aligned}
&u\Big|_{\bar{r}=1} = 0 \\
&v\Big|_{\bar{r}=1} = 0 \\
&u\Big|_{\bar{r}_R} \left(2 - \frac{\bar{p}_{FO}}{\bar{p}_{RO}} \right) = L_r \frac{du}{d\bar{r}}\Big|_{\bar{r}_R} - L_i \frac{dv}{d\bar{r}}\Big|_{\bar{r}_R} + F_r N_r \\
&\qquad + F_i N_i - 7 \bar{p}_{RO} (\bar{p}_{FO} - \bar{p}_{RO}) \\
&v\Big|_{\bar{r}=\bar{r}_R} \left(2 - \frac{\bar{p}_{FO}}{\bar{p}_{RO}} \right) = L_r \frac{dv}{d\bar{r}}\Big|_{\bar{r}_R} + L_i \frac{du}{d\bar{r}}\Big|_{\bar{r}_R} + F_r N_i - F_i N_r
\end{aligned}\right\} \tag{2.43}$$

The last two boundary conditions are derived from Eq.'s (2.32) and (2.34). The details of derivation and the definitions of L_r, L_i, F_r, etc., are shown in Appendix B.

In appendix C, Eq.'s (2.41) and (2.42) subject to boundary conditions (2.43) are solved numerically using matrix multiplication method (Ref. 8).

3. LOAD CAPACITY AND DYNAMIC BEARING REACTIONS

The pressure distribution in the thrust bearing under consideration can be summarized as follows:

i) The pressure in the feeding hole region is uniform and steady.

ii) The pressure inside the recessed pocket is uniform (approximately) but time-dependent.

iii) The pressure distribution in the film is

$$\bar{p}\ (\bar{r},\ \tau) = \bar{p}_o\ (\bar{r}) + \bar{\varepsilon}\ e^{i\tau}\ \frac{u + iv}{\bar{p}_o}$$

$$= \bar{p}\ (\bar{r}) + \bar{\varepsilon}\ \frac{u\ (\bar{r})\ \cos\tau - v\ (\bar{r})\ \sin\tau}{\bar{p}_o(r)} \qquad (3.1)$$

The bearing force may be obtained by integrating the pressure relative to the ambient, throughout the film. Thus,

$$W = \int_o^R (p - p_a)\ 2\pi r\ dr$$

$$= \pi r_F^2\ (p_s - p_a) + \pi(r_R^2 - r_F^2)(p_F - p_a) + 2\pi \int_{r_R}^R (p - p_a)\ r\ dr \qquad (3.2)$$

Non-dimensionalizing the load by $\pi R^2 p_a$, we have

$$W = \frac{W}{\pi R^2 p_a} = \bar{r}_F^2\ (\bar{p}_s - 1) + (\bar{r}_R^2 - \bar{r}_F^2)(\bar{p}_{FO} - 1 + \bar{\varepsilon}\ \bar{p}_{F1}\ e^{i\tau})$$

$$+ 2 \int_{\bar{r}_R}^1 (\bar{p}_o - 1 + \bar{\varepsilon}\ \bar{p}\ \ e^{i\tau})\ \bar{r}\ d\bar{r} \qquad (3.3)$$

Steady-State Load Capacity and Stiffness

In Eq. (3.3) the time-independent part alone contributes to the steady-state load capacity,

$$\frac{W_o}{\pi R^2 p_a} = \bar{r}_F^2\ (\bar{p}_s - 1) + (\bar{r}_R^2 - \bar{r}_F^2)(\bar{p}_{FO} - 1) + 2 \int_{\bar{r}_R}^1 (\bar{p}_o - 1)\ \bar{r}\ d\bar{r} \qquad (3.4)$$

This can be easily calculated with the aid of Eq. (2.21) and the solutions, $\bar{p}_{FO}$ and $\bar{p}_{RO}$, of Equations (2.37) and (2.38). From the load capacity, the static stiffness can be obtained by

$$\frac{Ck_o}{\pi R^2 p_a} = - C \frac{\partial}{\partial C}\left(\frac{W_o}{\pi R^2 p_a}\right) = - \frac{C}{2\Delta C}\left\{\frac{W_o^{(+)}}{\pi R^2 p_a} - \frac{W_o^{(-)}}{\pi R^2 p_a}\right\} \qquad (3.5)$$

where the superscripts (+) and (-) refer to load capacities at $C + \Delta C$ and $C - \Delta C$ respectively. ΔC should be sufficiently small; a suitable value for ΔC is $0.01C$.

Recall that in calculating the steady-state pressures, we have two parameters, namely, the geometry parameter Γ and the modified feeding parameter Λ_1.

In Figure 3, the dimensionless static stiffness $\frac{Ck_o}{\pi R^2 p_a}$ is plotted against Λ_1 for a bearing with $\frac{r_F}{R} = .002$, $\frac{r_R}{R} = 0.5$, $\frac{h_R}{C} = 2$ and $\Gamma = 1.736 \times 10^6$. It seems that for $\bar{p}_s = 2$, 3 and 4, the respective stiffness has a maximum value when Λ_1 is approximately 0.9. If we change the geometry to make $\Gamma = 1 \times 10^3$, numerical computation shows that the dimensionless stiffness falls fairly closely with the respective curves in Figure 3. This confirms the conclusion in the previous section that as long as Γ is large, the results should be insensitive to Γ.

Dynamic Bearing Reactions

The dynamic bearing reaction due to axial vibration is, from the time-dependent part of Eq. (3.3)

$$\frac{F_z}{\pi R^2 p_a} = \bar{\epsilon}\, \mathrm{Re}\left\{(\bar{r}_R^2 - \bar{r}_F^2)\, \bar{p}_{F1}\, e^{i\tau} + 2\int_{\bar{r}_R}^{1} \bar{p}_1\, e^{i\tau}\, \bar{r}\, d\bar{r}\right\}$$

$$= - \bar{\epsilon}\, \mathrm{Re}\left\{e^{i\tau}(U_z + i\, V_z)\right\} \qquad (3.6)$$

where

$$U_z = - (\bar{r}_R^2 - \bar{r}_F^2)\, (\bar{p}_{F1})_r - 2\int_{\bar{r}_R}^{1} \frac{u}{\bar{p}_o}\, \bar{r}\, d\bar{r}$$

$$= \text{Dynamic Stiffness} \qquad (3.7)$$

V_z = Dynamic Damping

$$= -(\bar{r}_R^2 - \bar{r}_F^2)(\bar{p}_{F1})_i - 2\int_{\bar{r}_R}^{1} \frac{v}{\bar{p}_o}\,\bar{r}\,d\bar{r} \tag{3.8}$$

Here u and v, the solutions of (2.41), (2.42) and (2.43), are solved numerically by the matrix-multiplication method as shown in Appendix C. Thus, the integrals in (3.7) and (3.8) can be calculated numerically. Using these results, the dynamic stiffness and damping are plotted against frequency in Figures 4 and 5 for different C. It is seen that when the frequency is low ($\omega \lesssim 1$) the dynamic stiffness approaches asymptotically to the value of the static stiffness and the dynamic damping approaches zero, as can be anticipated. When the frequency increases, the dynamic damping first decreases and reaches a minimum, then it starts to increase as shown in Figure 5. The frequency at which $V_z = 0$, is called the critical frequency. These will be useful in the stability analysis in the next section.

4. STABILITY

In the previous section, we have calculated the dynamic bearing reactions corresponding to small axial vibrations about the equilibrium (statically) position. These information are directly useful in determining the bearing stability.

In Reference 6, a stability analysis for either a single or two degree-of-freedom system was performed. The results for a single degree-of-freedom system are directly applicable; they may be stated as follows:

Let ν_o be the frequency of vibration at which

$$V_z\Big|_{\nu_o} = 0 \tag{4.1}$$

This is the state of neutral stability. Then, the critical mass is given by

$$M_o = \frac{P_a \pi R^2}{C\nu_o^2} \; U_z\Big|_{\nu_o} \tag{4.2}$$

A slight variation from the state of neutral stability would cause the system to be unstable if and only if

$$\frac{\partial V_z}{\partial \nu}\Big|_{\nu_o} \delta M > C \tag{4.3}$$

where δM is a small mass increment above M_o. From Figure 5, $\frac{\partial V_z}{\partial \nu}\Big|_{\nu_o} > 0$. Therefore, in order for the bearing to be stable, δM must be less than zero; or, the bearing mass must be kept below the critical mass.

Based on the above and a knowledge of U_z and V_z, the values of the critical mass were calculated from Eq. (4.2); they were shown in Figures 6, 7 and 8. Since we are dealing with bearings with subsonic flow throughout the passage and Vohr's data (Ref. 4) are essentially for low Mach number flows, we calculate the Mach number at $\bar{r} = \bar{r}_F$ using Eq. (2.12) to compute the velocity. The solid lines in Figures 3, 6, 7 and 8 are for Mach number $M < 0.9$. Those segments of the curves of Figs. 3, 6, 7 and 8 shown in dashed lines correspond to $M > 0.9$ and should be regarded with caution.

One of the stability maps (experimental data) of Ref. 2 is reproduced in Fig. 9 where the critical depth of the recessed pocket is plotted against the supply pressure.

The present analysis predicts a critical depth of 0.0011 in at p_s = 97.5 psia which is slightly below the experimental point in Figure 9. This indicates that the present method yields concervative stability result. This is believed to be in part due to the assumption of a uniform pressure in the recess pocket.

5. CONCLUSIONS

1. Vohr's entrance restriction data can be quite readily applied to analyze the externally pressurized thrust bearing with an inherently compensated restrictor. This analysis uncovers two controlling parameters, namely, the modified feeding parameter Λ_i and the geometry parameter Γ; the latter represents the relative degree of restriction between the exit of the feeding hole and the exit of the recessed pocket.

2. Steady-state load capacity and stiffness were calculated. It was found that the static stiffness has a maximum value when the modified feeding parameter Λ_i is approximately 0.9.

3. Applying the stability theory of Ref. 6, stability maps were constructed for a particular bearing geometry at different supply pressure. Experimental results of Ref. 2 were compared with the present analysis; it was found that the result of the present analysis is on the conservative side.

6. RECOMMENDATIONS

1. Use the well-known nozzle formula to replace the loss coefficient formulation, and then carry out the analysis. Compare the results.

2. Perform limit cycle analysis according to the scheme suggested in Appendix D.

3. Perform experiments to obtain more extensive data on loss coefficient at higher supply pressure. This will take the compressibility effects into account and thus, modify the results for bearings with high entrance Mach number (but still subsonic).

APPENDIX A

The Uniformity of Pressure in the Recessed Pocket

In writing the isothermal Reynolds' equation for the recessed pocket, it is more appropriate to nondimensionalize the radial coordinate by r_R and the gap by $C + h_R$. Thus, define

$$\tilde{r} = \frac{r}{r_R}$$

$$\tilde{h} = \frac{h + h_R}{C + h_R} \tag{A-1}$$

then the Reynolds' equation is

$$\frac{1}{\tilde{r}} \frac{\partial}{\partial \tilde{r}} \left[\tilde{r}\, \tilde{h}^3\, \bar{p}\, \frac{\partial \bar{p}}{\partial \tilde{r}} \right] = \tilde{\sigma}\, \frac{\partial}{\partial \tau} (\bar{p}\, \tilde{h}) \tag{A-2}$$

where $\tilde{\sigma}$ = Squeeze number for the pocket

$$= \frac{12\mu\omega}{p_a} \left(\frac{r_R}{C + h_R} \right)^2 \tag{A-3}$$

If $\tilde{\sigma}$ is much smaller than unity (this will be verified a postiori, after we calculate ω), then

$$\frac{1}{\tilde{r}} \frac{\partial}{\partial \tilde{r}} \left[\tilde{r}\, \tilde{h}^3\, \frac{\partial \bar{p}^2}{\partial \tilde{r}} \right] = 0 \tag{A-4}$$

or

$$\tilde{r}\, \tilde{h}^3\, \frac{\partial \bar{p}^2}{\partial \tilde{r}} = \text{const.} \tag{A-5}$$

The left hand side of Eq. (A-5) is essentially the mass flow rate through the bearing, which is constant everywhere under quasi-static condition ($\tilde{\sigma} \ll 1$). Therefore, we deduce that

$$\frac{\partial \bar{p}^2}{\partial \tilde{r}} \propto \frac{1}{\tilde{r}\, \tilde{h}^3} \tag{A-6}$$

Since h_R is greater than or at least equal to C, the gap of the pocket is at least twice of the bearing film thickness. Hence we conclude that, if $\tilde{\sigma} \ll 1$, then the gradient of $\bar{p}^2$ is much flatter in the pocket than that in the bearing film, or, the pressure in the recessed pocket can be assumed to be essentially uniform (spatially).

APPENDIX B

The Derivations of Boundary Conditions and the Pocket Perturbation Pressure

From Eq. (2.34), we can solve for $\bar{p}_{FI}$

$$\bar{p}_{Fl} = \frac{\dfrac{1 + 3\,\bar{h}_R}{1 + \bar{h}_R} + 6 + E\left[6\left.\dfrac{d(\bar{p}_o\,\bar{p}_l)}{d\bar{r}}\right|_{\bar{r}_R} - 3\,i\,\sigma\,\bar{p}_{FO}\,\dfrac{\bar{r}_R^{\,2} - \bar{r}_F^{\,2}}{\bar{r}_R}\right]}{F_r + i\,F_i} \tag{B.1}$$

where

$$F_r = -\frac{1}{\bar{p}_s - \bar{p}_{FO}} + \frac{1}{\bar{p}_{FO}}$$

$$F_i = 3\,\sigma\,E\,\frac{\bar{r}_R^{\,2} - \bar{r}_F^{\,2}}{\bar{r}_R}\,(1 + \bar{h}_R) \tag{B.2}$$

Or, we can write

$$\bar{p}_{Fl} = (\bar{p}_{Fl})_r + i\,(\bar{p}_{Fl})_i \tag{B.3}$$

if we denote

$$\left.\begin{aligned}
(\bar{p}_{Fl})_r &= \frac{\ell_r F_r + \ell_i F_i}{F_r^{\,2} + F_i^{\,2}} \\
(\bar{p}_{Fl})_i &= \frac{-\ell_r F_i + \ell_i F_r}{F_r^{\,2} + F_i^{\,2}} \\
\ell_r &= 6\,E\left.\frac{du}{d\bar{r}}\right|_{\bar{r}_R} + \frac{1 + 3\,\bar{h}_R}{1 + \bar{h}_R} + 6 \\
\ell_i &= 6\,E\left.\frac{dv}{d\bar{r}}\right|_{\bar{r}_R} - 3\,\sigma\,E\,\bar{p}_{FO}\,\frac{\bar{r}_R^{\,2} - \bar{r}_F^{\,2}}{\bar{r}_R}
\end{aligned}\right\} \tag{B.4}$$

Substituting (B.1) into (2.32) and solving for $\bar{p}_{R1}$ we obtain

$$\left(2 - \frac{\bar{p}_{FO}}{\bar{p}_{RO}}\right) \bar{p}_{R1} = \left(\frac{1}{F_r + i\,F_i} - \bar{p}_{FO} + \bar{p}_{RO}\right) 6\,E\,\frac{d}{d\bar{r}}\,(\bar{p}_o\,\bar{p}_1)\Big|_{\bar{r}_R}$$

$$+ \frac{1}{F_r + i\,F_i}\left[\frac{1 + 3\,\bar{h}_R}{1 + \bar{h}_R} + 6 - 3\,i\,\sigma\,E\,\bar{p}_{FO}\,\frac{\bar{r}_R^{\,2} - \bar{r}_F^{\,2}}{\bar{r}_R}\right]$$

$$- 7\,(\bar{p}_{FO} - \bar{p}_{RO})$$

Multiply both sides by $\bar{p}_{RO}$

$$\left(2 - \frac{\bar{p}_{FO}}{\bar{p}_{RO}}\right)(\bar{p}_{RO}\,\bar{p}_{R1}) = 6\,E\left(\frac{F_r - i\,F_i}{F_r^{\,2} + F_i^{\,2}} - \bar{p}_{FO} + \bar{p}_{RO}\right)\left(\frac{du}{d\bar{r}} + i\,\frac{dv}{d\bar{r}}\right)\Big|_{\bar{r}_R}$$

$$+ \frac{\bar{p}_{RO}}{F_r^{\,2} + F_i^{\,2}}\left\{\left[\left(\frac{1 + 3\,\bar{h}_R}{1 + \bar{h}_R} + 6\right) F_r + \left(-3\,\sigma\,E\,\bar{p}_{FO}\,\frac{\bar{r}_R^{\,2} - \bar{r}_F^{\,2}}{\bar{r}_R}\right) F_i\right]\right.$$

$$\left. - i\left[\left(\frac{1 + 3\,\bar{h}_R}{1 + \bar{h}_R} + 6\right) F_i + 3\,\sigma\,E\,\bar{p}_{FO}\,\frac{\bar{r}_R^{\,2} - \bar{r}_F^{\,2}}{\bar{r}_R}\,F_r\right]\right\} - 7\,\bar{p}_{RO}\,(\bar{p}_{FO} - \bar{p}_{RO}) \qquad (B.5)$$

The product $\bar{p}_{RO}\,\bar{p}_{R1}$ can be written as

$$\bar{p}_{RO}\,\bar{p}_{R1} = (\bar{p}_o\,\bar{p}_1)_{\bar{r}_R} = (u + iv)_{\bar{r}_R} \qquad (B.6)$$

Now let us define

$$\left.\begin{aligned}
L_r &= \left(\frac{F_r}{F_r^{\,2} + F_i^{\,2}} - \bar{p}_{FO} + \bar{p}_{RO}\right) 6\,E\,\bar{p}_{RO} \\
L_i &= -\frac{F_i}{F_r^{\,2} + F_i^{\,2}}\,6\,E\,\bar{p}_{RO} \\
N_r &= \left(\frac{1 + 3\,\bar{h}_R}{1 + \bar{h}_R} + 6\right)\frac{\bar{p}_{RO}}{F_r^{\,2} + F_i^{\,2}} \\
N_i &= -3\,\sigma\,E\,\bar{p}_{FO}\,\frac{\bar{r}_R^{\,2} - \bar{r}_F^{\,2}}{\bar{r}_R}\,\frac{\bar{p}_{RO}}{F_r^{\,2} + F_i^{\,2}}
\end{aligned}\right\} \qquad (B.7)$$

then Eq. (B.5) becomes

$$\left(2 - \frac{\bar{p}_{FO}}{\bar{p}_{RO}}\right)(u + i\,v)\Big|_{\bar{r}_R} = \left[L_r \frac{du}{d\bar{r}}\Big|_{\bar{r}_R} - L_i \frac{dv}{d\bar{r}}\Big|_{\bar{r}_R} + i\left(L_r \frac{dv}{d\bar{r}}\Big|_{\bar{r}_R} + L_i \frac{du}{d\bar{r}}\Big|_{\bar{r}_R}\right)\right]$$

$$+ \left[F_r N_r + F_i N_i + i(F_r N_i - F_i N_r)\right]$$

$$- 7\,\bar{p}_{RO}\,(\bar{p}_{FO} - \bar{p}_{RO}) \qquad (B.8)$$

Separating the real and imaginary parts, we obtain easily the following boundary conditions

$$u\Big|_{\bar{r}_R}\left(2 - \frac{\bar{p}_{FO}}{\bar{p}_{RO}}\right) = L_r \frac{du}{d\bar{r}}\Big|_{\bar{r}_R} - L_i \frac{dv}{d\bar{r}}\Big|_{\bar{r}_R} + z_1 \qquad (B.9)$$

$$v\Big|_{\bar{r}_R}\left(2 - \frac{\bar{p}_{FO}}{\bar{p}_{RO}}\right) = L_r \frac{dv}{d\bar{r}}\Big|_{\bar{r}_R} + L_i \frac{du}{d\bar{r}}\Big|_{\bar{r}_R} + z_2 \qquad (B.10)$$

where

$$z_1 = F_r N_r + F_i N_i - 7\,\bar{p}_{RO}\,(\bar{p}_{FO} - \bar{p}_{RO})$$

$$z_2 = F_r N_i - F_i N_r \qquad (B.11)$$

Pocket Perturbation Pressure

The perturbation pressure at the pocket $\bar{p}_{F1}$ can be calculated from Equations (B.3) and (B.4). However, it is important to note that, when the frequency is very low, $F_i \tilde{\sim} 0$, (in the limit of zero frequency, $F_i = 0$; this corresponds to a static perturbation) and from Eq. (B.4) we have

$$(\bar{p}_{F1})_r \tilde{\sim} \frac{\ell_r F_r}{F_r^2} = \frac{\ell_r}{F_r} \qquad (B.12)$$

For a given geometry and a supply pressure, by varying the equilibrium film thickness one would obtain a steady-state pocket pressure equal to one half the supply pressure at a particular value of C. It is obvious from Equation (B.2) that when

$\bar{P}_{FO} = \frac{1}{2}\bar{P}_s$,

$$F_r = 0 \tag{B.13}$$

Equations (B.12) and (B.13) indicate that under the given supply pressure, $(\bar{P}_{F1})_r$ has a singular behavior. It can be shown, however, by a static perturbation analysis, that whenever $F_r = 0$, $\ell_r = 0$. Therefore, the singularity is probably a removable one, i.e., the ratio ℓ_r/F_r will approach a definite value. (One can argue that physically $(\bar{P}_{F1})_r$ should approach a definite value). But, the above computation for $(\bar{P}_{F1})_r$ cannot be programmed on a computer because it is unlikely that the machine will give us the correct limiting value.

One way to avoid the above situation is to calculate $\bar{P}_{FI}$ by using Equation (2.32),

$$\bar{P}_{F1} = \bar{P}_{R1} + (\bar{P}_{FO} - \bar{P}_{RO})\left\{7 - \frac{\bar{P}_{R1}}{\bar{P}_{RO}} + 6E\left(\left.\frac{du}{d\bar{r}}\right|_{\bar{r}_R} + i\left.\frac{dv}{d\bar{r}}\right|_{\bar{r}_R}\right)\right\} \tag{B.14}$$

Recall that $$\bar{P}_{R1} = \frac{1}{\bar{P}_{RO}}\left(u\Big|_{\bar{r}_R} + i\,v\Big|_{\bar{r}_R}\right) \tag{B.15}$$

Thus, we obtain

$$\begin{aligned}(\bar{P}_{F1})_r &= \frac{1}{\bar{P}_{RO}}\left(2 - \frac{\bar{P}_{FO}}{\bar{P}_{RO}}\right)u\Big|_{\bar{r}_R} + (\bar{P}_{FO} - \bar{P}_{RO})\left(7 + 6E\left.\frac{du}{d\bar{r}}\right|_{\bar{r}_R}\right)\\ (\bar{P}_{F1})_i &= \frac{1}{\bar{P}_{RO}}\left(2 - \frac{\bar{P}_{FO}}{\bar{P}_{RO}}\right)v\Big|_{\bar{r}_R} + (\bar{P}_{FO} - \bar{P}_{RO})\left(6E\left.\frac{dv}{d\bar{r}}\right|_{\bar{r}_R}\right)\end{aligned} \tag{B.16}$$

APPENDIX C

The Matrix Multiplication Method in Solving Ordinary Differential Equations with "Two-Point" Boundary Conditions*

Equations (2.41) and (2.42) together with their boundary conditions (2.43) may be written in the following general form:

$$\text{D.E.} \begin{cases} u'' + f_1 u' + f_2 u + f_3 v'' + f_4 v' + f_5 v = f_6 & \text{(C.1)} \\ v'' + g_1 v' + g_2 v + g_3 u'' + g_4 u' + g_5 u = g_6 & \text{(C.2)} \end{cases}$$

$$\text{B.C.} \begin{cases} \text{at } x = x_1, \quad u = c_1 u' + c_2 v' + c_3, \quad v = c_4 u' + c_5 v' + c_6 & \text{(C.3)} \\ \text{at } x = x_2, \quad u = \bar{F}, \quad v = \bar{G} & \text{(C.4)} \end{cases}$$

Here we denote the independent variable by x. The primes represent derivatives with respect to x. The symbols f_1, f_2, . . . etc., are known functions of x; c_1, c_2, . . . etc., are known constants.

In central difference form, we can write

$$\left.\begin{aligned} u(x_k) &= u^k \\ u'(x_k) &= \frac{u^{k+1} - u^{k-1}}{2\Delta} \\ u''(x_k) &= \frac{u^{k+1} - 2u^k + u^{k-1}}{\Delta^2} \end{aligned}\right\} \qquad \text{(C.5)}$$

We have assumed that there are N divisions between x_1 and x_2, so that k = 0, 1, 2, . . N, and $\Delta = \frac{x_2 - x_1}{N}$

Now, Eq. (A.1) take the form

$$u^{k+1}\left[\frac{1}{\Delta^2} + \frac{f_1^k}{2\Delta}\right] + u^k\left[\frac{-2}{\Delta^2} + f_2^k\right] + u^{k-1}\left[\frac{1}{\Delta^2} - \frac{f_1^k}{2\Delta}\right]$$
$$+ v^{k+1}\left[\frac{f_3^k}{\Delta^2} + \frac{f_4^k}{2\Delta}\right] + v^k\left[\frac{-2f_3^k}{\Delta^2} + f_5^k\right] + v^{k-1}\left[\frac{f_3^k}{\Delta^2} - \frac{f_4^k}{2\Delta}\right] = f_6^k \qquad \text{(C.6)}$$

---

*The method of computation described in this appendix is due to Castelli and Pirvics (Ref. 8).

A similar equation may be obtained from Eq. (C.2), which together with (C.6) can be written in the following matrix form,

$$A^k\, y^{k+1} + B^k\, y^k + C^k\, y^{k-1} = d^k \tag{C.7}$$

where

$$\left.\begin{aligned}
y^{(\,)} &= \begin{bmatrix} u^{(\,)} \\ v^{(\,)} \end{bmatrix} \\
A^k &= \begin{bmatrix} \frac{1}{\Delta^2} + \frac{f_1{}^k}{2\Delta} & \frac{f_3{}^k}{\Delta^2} + \frac{f_4{}^k}{2\Delta} \\ \frac{g_3{}^k}{\Delta^2} + \frac{g_4{}^k}{2\Delta} & \frac{1}{\Delta^2} + \frac{g_1{}^k}{2\Delta} \end{bmatrix} \\
B^k &= \begin{bmatrix} \frac{-2}{\Delta^2} + f_2{}^k & \frac{-2f^k}{\Delta^2} + f_5{}^k \\ \frac{-2g_3{}^k}{\Delta^2} + g_3{}^k & \frac{-2}{\Delta^2} + g_2{}^k \end{bmatrix} \\
C^k &= \begin{bmatrix} \frac{1}{\Delta^2} - \frac{f_1{}^k}{2\Delta} & \frac{f_3{}^k}{\Delta^2} - \frac{f_4{}^k}{2\Delta} \\ \frac{g_3{}^k}{\Delta^2} - \frac{g_4{}^k}{2\Delta} & \frac{1}{\Delta^2} - \frac{g_1{}^k}{2\Delta} \end{bmatrix} \\
d^k &= \begin{bmatrix} f_6{}^k \\ g_6{}^k \end{bmatrix}
\end{aligned}\right\} \tag{C.8}$$

Assume that the y-vector at station "k + 1" can be expressed by

$$y^{k+1} = M^k\, y^k + m^k \tag{C.9}$$

where M is an unknown matrix and m, an unknown vector. From (C.9) we can write formally

$$\left.\begin{aligned} y^k &= M^{k-1}\, y^{k-1} + m^{k-1} \\ \text{and} \\ y^{k-1} &= M^{k-2}\, y^{k-2} + m^{k-2} \end{aligned}\right] \qquad \text{(C.10)}$$

Substitute (C.9) and (C.10) into (C.7),

$$(A^k M^k + B^k)\, y^k + C^k\, y^{k-1} = d^k - A^k\, m^k$$

Thus,

$$y^k = [A^k M^k + B^k]^{-1}\, [-C^k\, y^{k-1} + (d^k - A^k\, m^k)] \qquad \text{(C.11)}$$

Comparing (C.11) with the first equation of (C.10), we find

$$M^{k-1} = [A^k M^k + B^k]^{-1}\, [-C^k] \qquad \text{(C.12)}$$

$$m^{k-1} = [A^k M^k + B^k]^{-1}\, (d^k - A^k\, m^k) \qquad \text{(C.13)}$$

Using (C.4)

$$y^N = \begin{bmatrix} \overline{F} \\ \overline{G} \end{bmatrix} \qquad \text{(C.14)}$$

and from the first equation of (C.10) we obtain

$$M^{N-1} = 0 \qquad \text{(C.15)}$$

$$m^{N-1} = \begin{bmatrix} \overline{F} \\ \overline{G} \end{bmatrix} \qquad \text{(C.16)}$$

Now we can use (C.12) and (C.13) as recurrance formulas to obtain

$$\left.\begin{aligned} M^{N-2} &= \left[A^{N-1}\, M^{N-1} + B^{N-1}\right]^{-1} \left[-C^{N-1}\right] \\ m^{N-2} &= \left[A^{N-1}\, M^{N-1} + B^{N-1}\right]^{-1} \left[d^{N-1} - A^{N-1}\, m^{N-1}\right] \end{aligned}\right] \qquad \text{(C.17)}$$

$$\left.\begin{aligned} M^{N-3} &= \left[A^{N-2}\, M^{N-2} + B^{N-2}\right]^{-1} \left[-C^{N-2}\right] \\ m^{N-3} &= \left[A^{N-2}\, M^{N-2} + B^{N-2}\right]^{-1} \left[d^{N-2} - A^{N-2}\, m^{N-2}\right] \end{aligned}\right] \qquad \text{(C.18)}$$

and so on.

Having computed the M's and m's, we can calculate the solution by marching from $x = x_1$ but first let us rewrite boundary condition (C.3).

$$u^o = C_1 \ (u^1 - u^o) + C_2 \ (v^1 - v^o) + C_3$$

$$v^o = C_1 \ (u^1 - u^o) + C_5 \ (v^1 - v^o) + C_6$$

using forward difference formula. In matrix form the above two equations can be written as

$$S \ y^o = T \ y^1 + z \tag{C.19}$$

where

$$\left.\begin{aligned} S &= \begin{bmatrix} 1 + C_1 & C_2 \\ 1 + C_4 & C_5 \end{bmatrix} \\ T &= \begin{bmatrix} C_1 & C_2 \\ C_4 & C_5 \end{bmatrix} \\ z &= \begin{bmatrix} z_1 \\ z_2 \end{bmatrix} \end{aligned}\right\} \tag{C.20}$$

Using the relationship

$$y^1 = M^o \ y^o + m^o \tag{C.21}$$

Equation (C.19) becomes

$$[S] \ y^o = [T][M^o] \ y^o + [T] \ m^o + z \tag{C.22}$$

Thus, we have finally

$$y^o = [S - T \ M^o]^{-1} \ (T \ m^o + z) \tag{C.23}$$

Now we can march from this point to obtain the solution, using Eq. (C.9),

$$\left.\begin{aligned} y^1 &= M^0\, y^0 + m^0 \\ y^2 &= M^1\, y^1 + m^1 \end{aligned}\right\} \qquad (C.24)$$

and so on.

APPENDIX D

Scheme for Limit Cycle Analysis

Let us symbolically write the Reynold's equation in the form:

$$R\left\{\bar{p}\right\} = \frac{1}{\bar{r}}\frac{\partial}{\partial\bar{r}}\left[\bar{r}\,\bar{h}^{3}\,\bar{p}\,\frac{\partial\bar{p}}{\partial\bar{r}}\right] - \sigma\frac{\partial}{\partial\tau}(\bar{p}\,\bar{h}) = 0 \tag{D.1}$$

Suppose that the bearing is unstable so that the amplitude of oscillation becomes larger and larger. Now, let us assume that a limit cycle motion will be reached and during the limit cycle motion (finite amplitude), the gap variation and pressure fluctuation remain to be sinusoidal. Thus,

$$\bar{h} = 1 + \bar{\epsilon}\cos\nu t \tag{D.2}$$

$$\bar{p} = \bar{p}_{o} + p_{1}(\bar{r})\cos\nu t + q_{1}(\bar{r})\sin\nu t \tag{D.3}$$

Here, the dimensionless amplitude $\bar{\epsilon}$ is not necessarily small.

Apply cosine and sine transforms to (D.1).

$$R_{c}\left\{p_{1}, q_{1}; \nu\right\} = \int_{-\pi/\nu}^{\pi/\nu} R\left\{p\right\}\cos\nu t\,dt = 0 \tag{D.4}$$

$$R_{s}\left\{p_{1}, q_{1}; \nu\right\} = \int_{-\pi/\nu}^{\pi/\nu} R\left\{p\right\}\sin\nu t\,dt = 0 \tag{D.5}$$

Note that a typical quantity in (D.1), $\bar{h}^{3}$, is equal to

$$\bar{h}^{3} = (1 + \bar{\epsilon}\cos\nu t)^{3}$$

$$= 1 + 3\bar{\epsilon}\cos\nu t + 3\bar{\epsilon}^{2}\cos^{2}\nu t + \bar{\epsilon}^{3}\cos^{3}\nu t \tag{D.6}$$

Utilizing the identities

$$\cos^2 \nu t = \tfrac{1}{2} (1 + \cos 2\nu t)$$

$$\cos^3 \nu t = \tfrac{1}{4} (3 \cos \nu t + \cos 3\nu t)$$

$$\int_{-\pi/\nu}^{\pi/\nu} \cos m\nu t \cos n\nu t \, dt = \pi \delta_{mn}$$

$$\int_{-\pi/\nu}^{\pi/\nu} \cos m\nu t \sin n\nu t \, dt = 0$$

$$\int_{-\pi/\nu}^{\pi/\nu} \sin m\nu t \sin n\nu t \, dt = \pi \delta_{mn}$$

etc., one realizes that (D.4) and (D.5) are two non-linear ordinary differential equations in p_1 and q_1, which are truncated to include only the simple harmonics.

Similarly we can carry out the cosine and sine transforms to the boundary conditions and mass conservation in the recessed pocket and so on. This would yield boundary conditions for the non-linear differential equations (D.4) and (D.5). Iteration method may be used in solving the non-linear system.

Having solved p_1 and q_1 we can compute the bearing forces.

$$W = 2\pi \int_0^R (p - p_a) \, r \, dr = W_o + U \cos \nu t + V \sin \nu t \qquad (D.7)$$

Then, the power output of the gas film, E, is

$$E = W \frac{\partial h}{\partial t} \qquad (D.8)$$

where $\frac{\partial h}{\partial t}$ is obviously the squeeze velocity.

The average power output over a squeeze cycle can be readily obtained by

$$\tilde{E} = \frac{\nu}{2\pi} \int_{-\pi/\nu}^{\pi/\nu} E \, dt = \frac{\nu}{2\pi} \int_{-\pi/\nu}^{\pi/\nu} W \frac{\partial h}{\partial t} \, dt$$

$$= \frac{\nu}{2\pi} \left(-\bar{\epsilon} C \nu\right) \int_{-\pi/\nu}^{\pi/\nu} W \sin \nu t \, dt$$

$$= -\frac{\nu \bar{\epsilon} C}{2} V(\bar{\epsilon}, \nu) \qquad (D.9)$$

Let the bearing mass be M and write the equation of motion

$$M \frac{d^2 h}{dt^2} + U \cos \nu t + V \sin \nu t = F \sin \nu t \qquad (D.10)$$

where F sin νt is the external force acting on the bearing other than the gas film forces.

Since $\frac{d^2 h}{dt^2} = -\bar{\epsilon} C \nu^2 \cos \nu t$, by collecting the cosine terms in (D.10) we obtain

$$-\bar{\epsilon} C \nu^2 M + U = \qquad (D.11)$$

Note that U is a function of ν and $\bar{\epsilon}$. Therefore, (D.11) is a highly non-linear equation. From equation (D.11) the natural frequency, ν_o, can be determined using numerical methods. In general, ν_o is a function of $\bar{\epsilon}$ and M. Thus,

$$\nu_o = \nu_o(\bar{\epsilon}, M) \qquad (D.12)$$

Having determined the natural frequency, a stability criterion can be established by energy consideration. The bearing is stable if $\tilde{E}$ is negative, and unstable if $\tilde{E}$ is positive. From Equation (D.9) we conclude that the bearing is stable if V is positive, and unstable if V is negative.

Now, at $\nu = \nu_o$,

$$V(\bar{\epsilon},\nu)\Big|_{\nu_o} = V\left(\bar{\epsilon},\nu_o(\bar{\epsilon},M)\right) = V(\bar{\epsilon},M) \tag{D.13}$$

A qualitative plot of V versus $\bar{\epsilon}$ for a given M is believed to be that shown in the diagram. The bearing is unstable when $\bar{\epsilon}$ is small. Hence the amplitude will

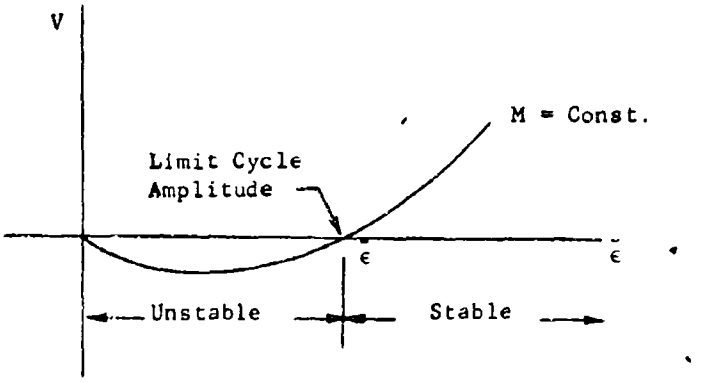

grow until it reaches a value, $\bar{\epsilon}_o$, where V = 0, and the bearing becomes marginally stable. The bearing is then said to reach a limit cycle motion with limit cycle amplitude $\bar{\epsilon}_o$.

NOMENCLATURE

C	equilibrium film thickness
d_F	diameter of feeding hole
d_R	diameter of recessed pocket
E	defined in (2.27)
F_r, F_i	defined in (B.2)
F_z	dynamic bearing reaction
G	mass flow rate per unit length
h	film thickness
h_R	depth of recessed pocket
$\bar{h}$	h/C
i	$\sqrt{-1}$
k_o	static stiffness
K'	loss coefficient = K Re
L_r, L_i	defined in (B.7)
ℓ_r, ℓ_i	defined in (B.4)
L	typical length
M	mass; matrix defined in (C.9)
N_r, N_i	defined in (B.7)
p	pressure
p_s	supply pressure
p_a	ambiant pressure
$\bar{p}$	dimensionless pressure
$\bar{p}_o, \bar{p}_i$	defined in (2.15)
Q_1	defined in (2.35)
r	radial coordinate
$\bar{r}$	dimensionless radial coordinate, r/R
r_F	radius of feeding hole
r_R	radius of recessed pocket
R	bearing radius
Re	Reynolds' number = $\frac{\rho V L}{\mu}$
$\bar{\text{Re}}$	Film entrance Reynolds' number = $\frac{\dot{m}}{\pi r_F \mu} = 2\frac{\rho V L}{\mu}$
R	gas constant
T	temperature
t	time

U_z	dynamic stiffness
V_z	dynamic damping
u, v	defined in (2.40)
V	velocity
W	bearing load
W_o	static load
y	
z	$[z_1, z_2]$ defined in (B.11)
Γ	geometry parameter defined in (2.36)
ε	amplitude of axial vibration
$\bar{\varepsilon}$	dimensionless ε
Λ_i	modified feeding parameter defined in (2.39)
μ	viscosity
ρ	density
σ	squeeze number defined in (2.5)
τ	dimensionless time
ω	frequency

REFERENCES

1. Licht, L., Fuller, D.D., and Sternlicht, B., "Self-Excited Vibration of an Air-Lubricated Thrust Bearing," Trans. ASME, vol. 80, p.411, 1958.

2. Licht, L., and Elrod, H.G., Jr., "An Analytical and Experimental Study of the Stability of Externally Pressurized, Gas-Lubricated Thrust Bearings," The Franklin Institute, Report No. 1-A2049-12, 1961.

3. Lund, J., Wernick, R.J., and Malanoski, S.B., "Analysis of the Hydrostatic Journal and Thrust Gas Bearing for the NASA AB-5 Gyro Gimbal Bearing," MTI Technical Report 62TR26, 1962.

4. Vohr, J., "An Experimental Study of Flow Phenomena in the Feeding Region of an Externally Pressurized Gas Bearing," MTI Technical Report 65TR47, 1965.

5. Carfagno, S.P., and McCabe, J.T., "Summary of Investigations of Entrance Effects in Circular Thrust Bearings," Franklin Institute Research Laboratories Interim Report 1-A2049, 1965.

6. Pan, C.H.T., "Spectral Analysis of Gas bearing Systems for Stability Studies," presented at the Ninth Midwestern Mechanics Conference, University of Wisconsin, Madison, Wis., August, 1965.

7. Ralston, A., and Wilf, H.S., "Mathematical Methods for Digital Computers," John Wiley & Sons, Inc., New York, N.Y., 1960.

8. Castelli, V., and Pirvics, J., "Equilibrium Characteristics of Axial-Groove Gas Lubricated Bearings," ASLE-ASME-ASLE Lubrication Conference, San Francisco, California, October, 1965.

9. Hildebrand, F.B., "Introduction to Numerical Analysis," McGraw-Hill Co., New York, N.Y., 1956.

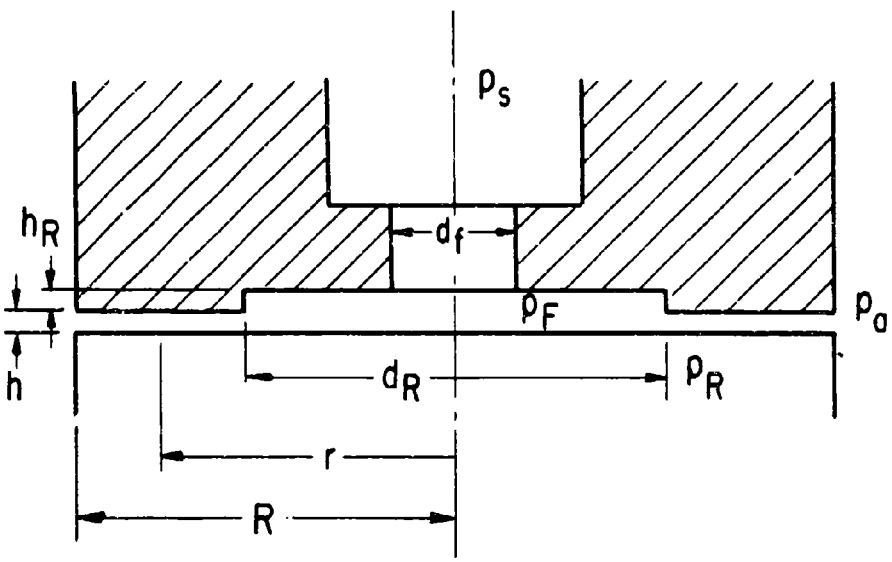

Fig. 1 Geometry of an Inherently Compensated, Hydrostatic, Circular, Thrust Bearing

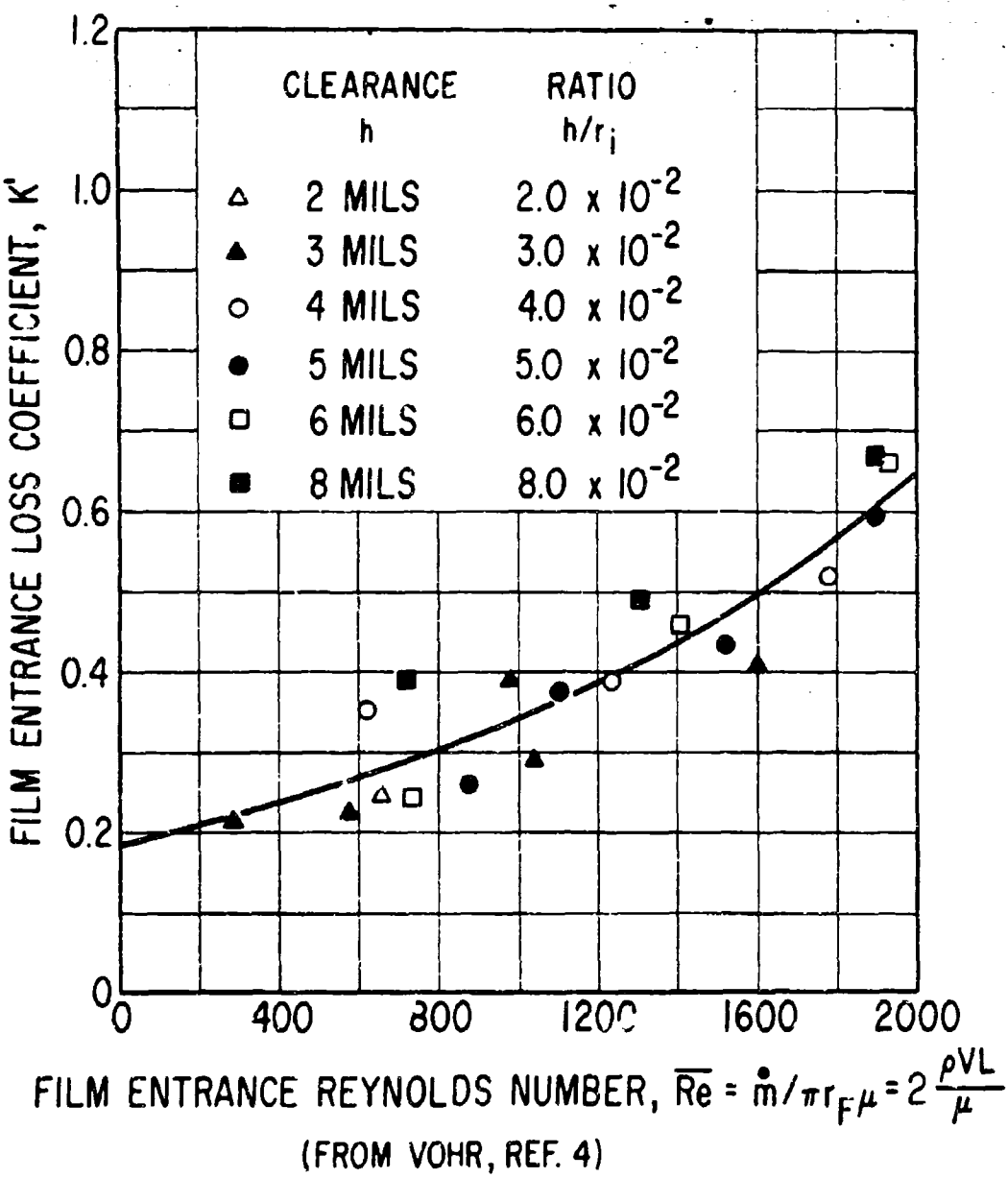

Fig. 2 Loss Coefficient versus Film Entrance Reynolds Number

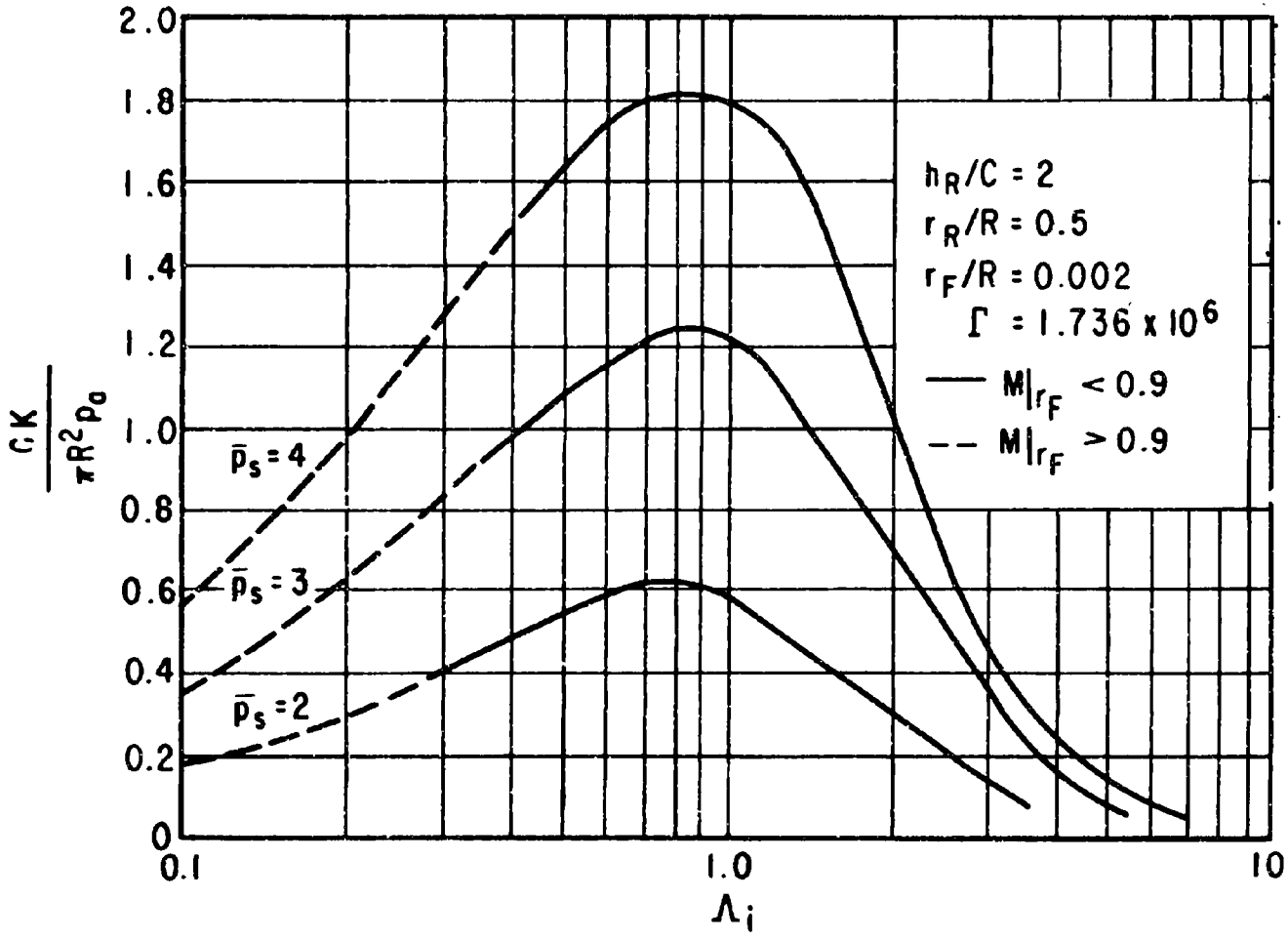

Fig. 3 Static Stiffness versus Λ_i

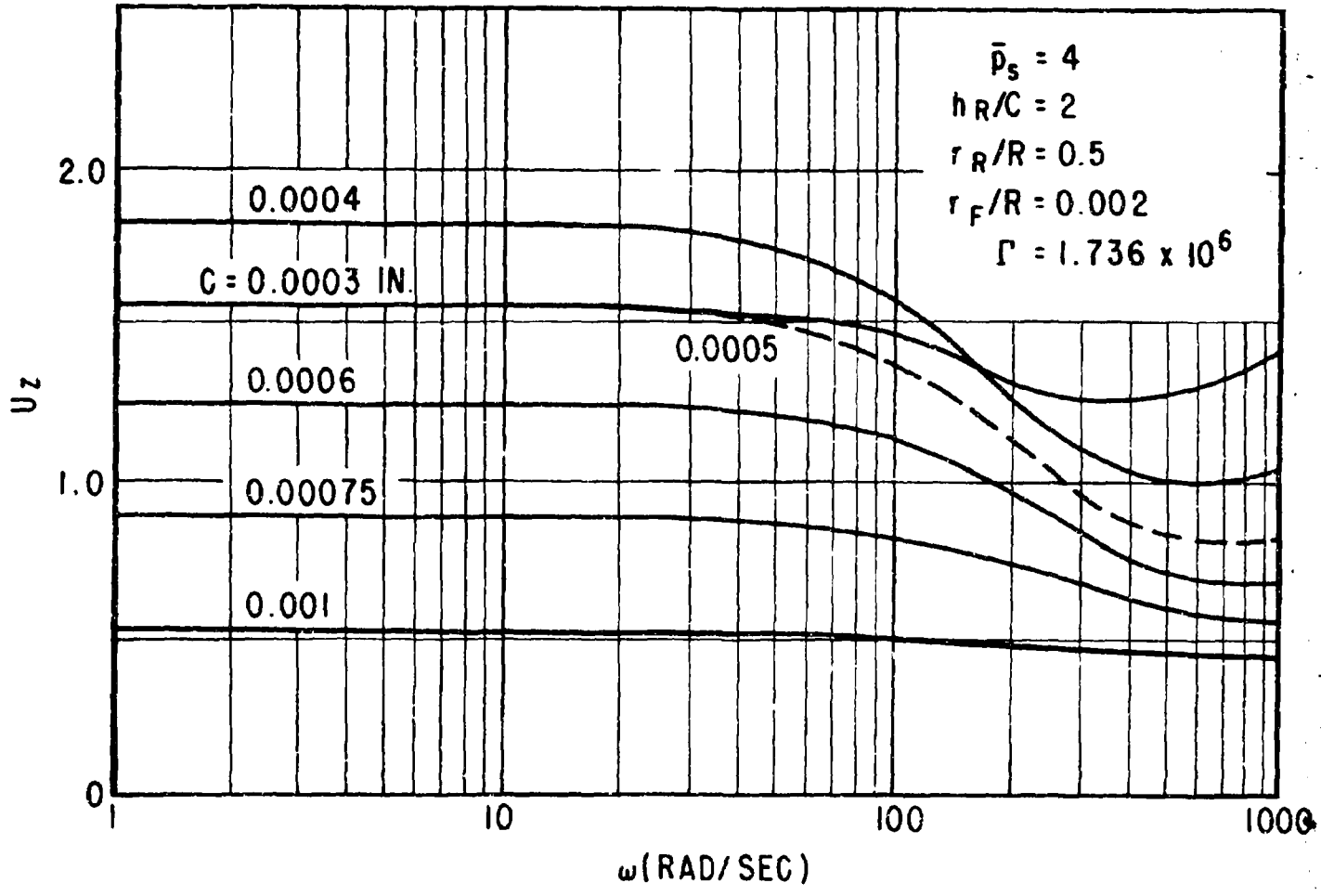

Fig. 4 Dynamic Stiffness U_z versus Frequency ω.

MIT-2555

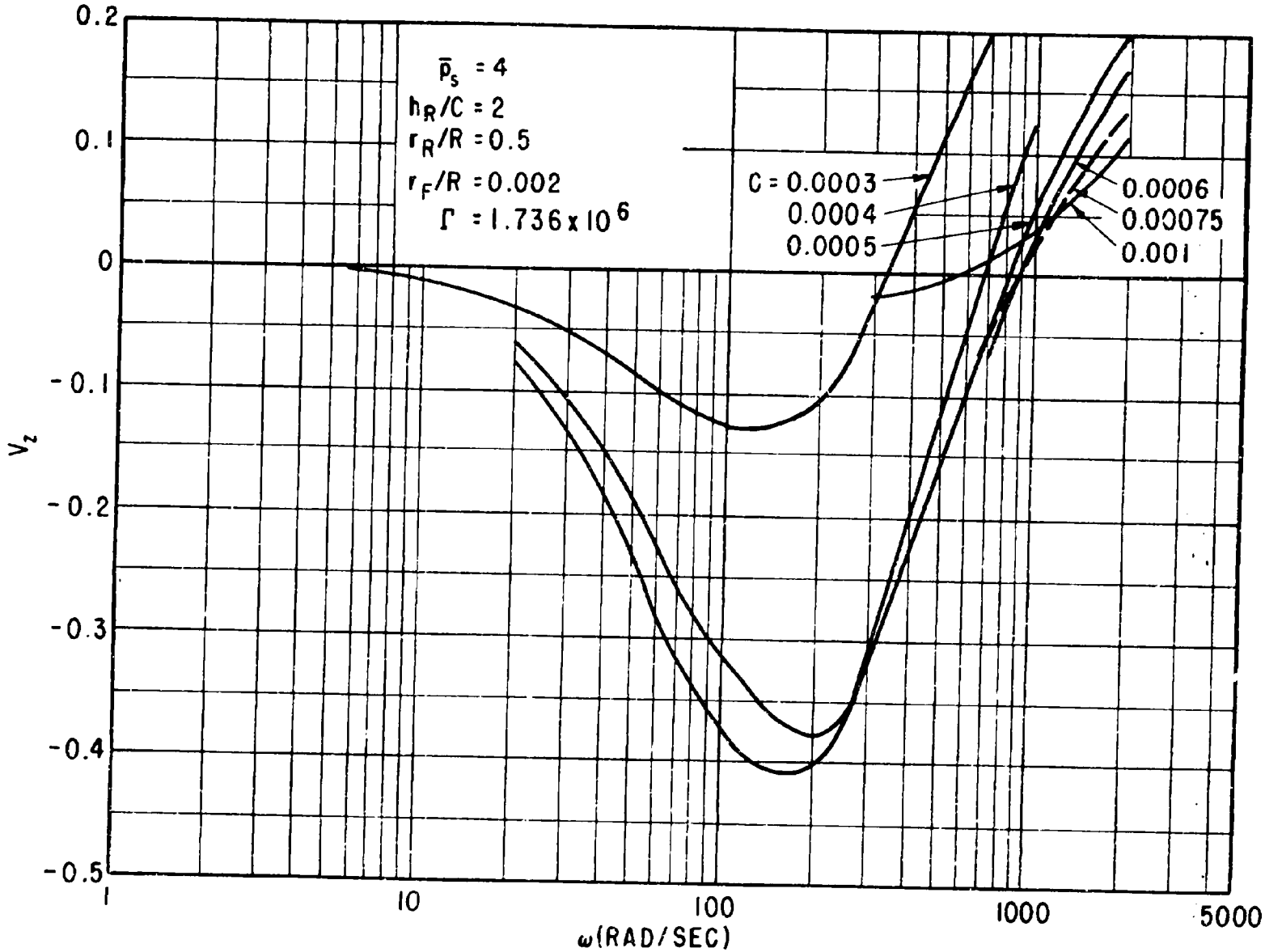

Fig. 5 Dynamic Damping V_z versus Frequency ω.

MTI-2555

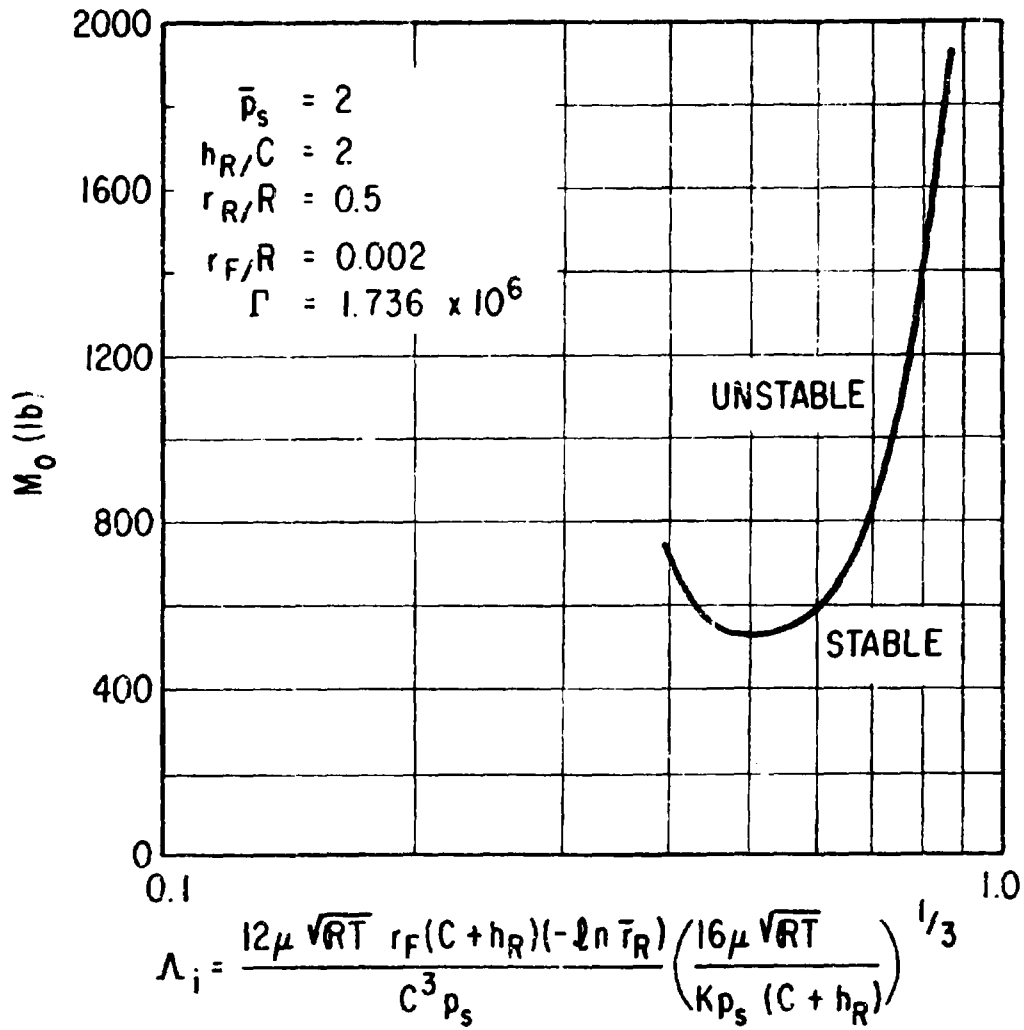

Fig. 6 Critical Mass versus Λ_i.

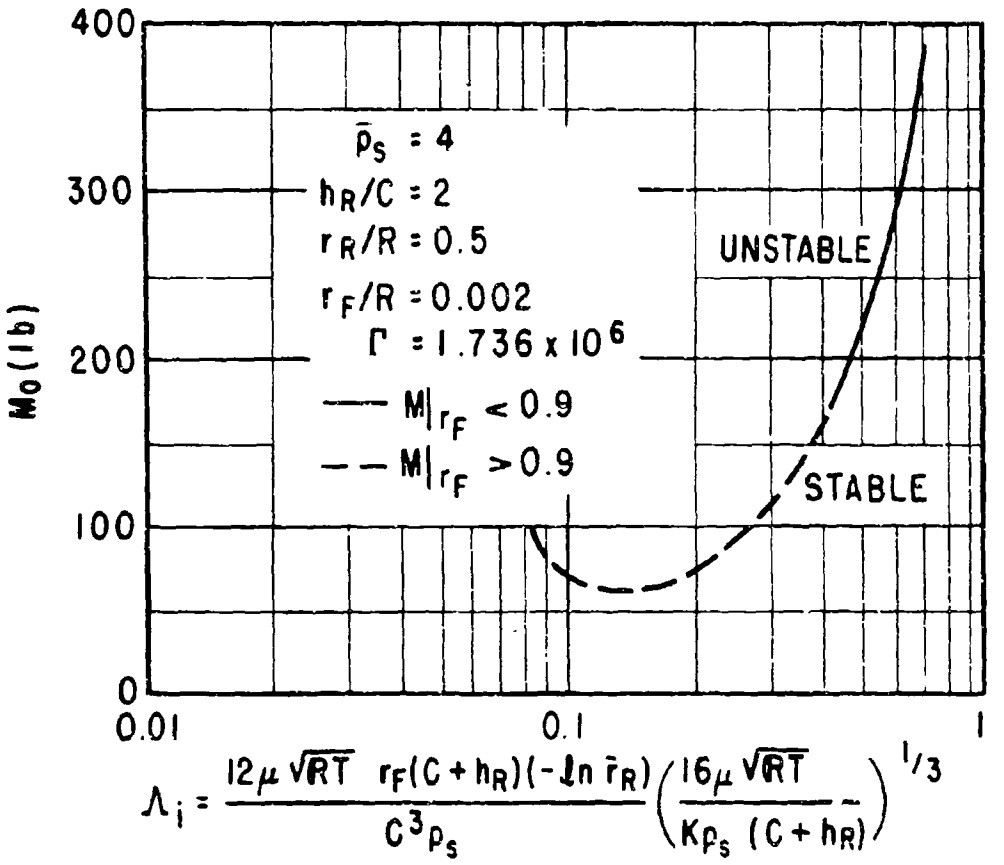

Fig. 7 Critical Mass versus Λ_i.

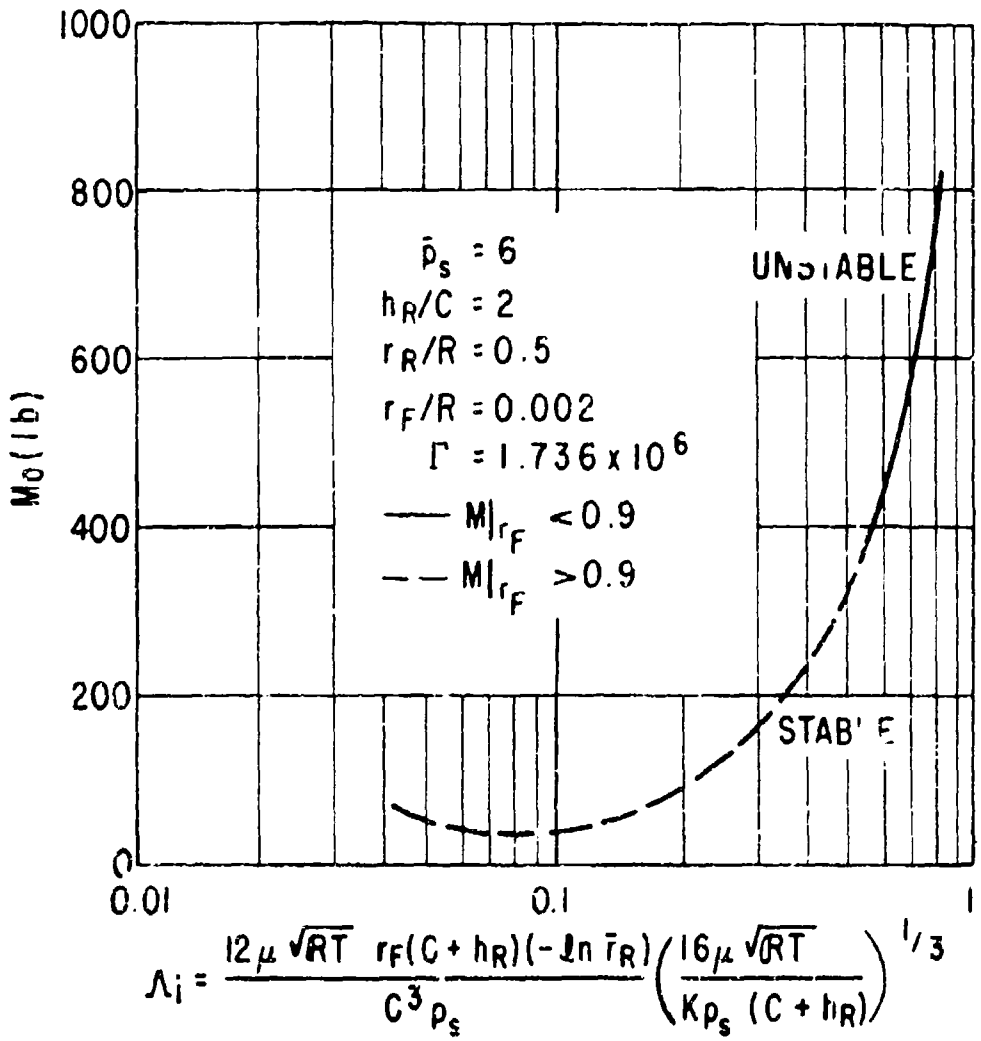

Fig. 8 Critical Mass versus Λ_i.

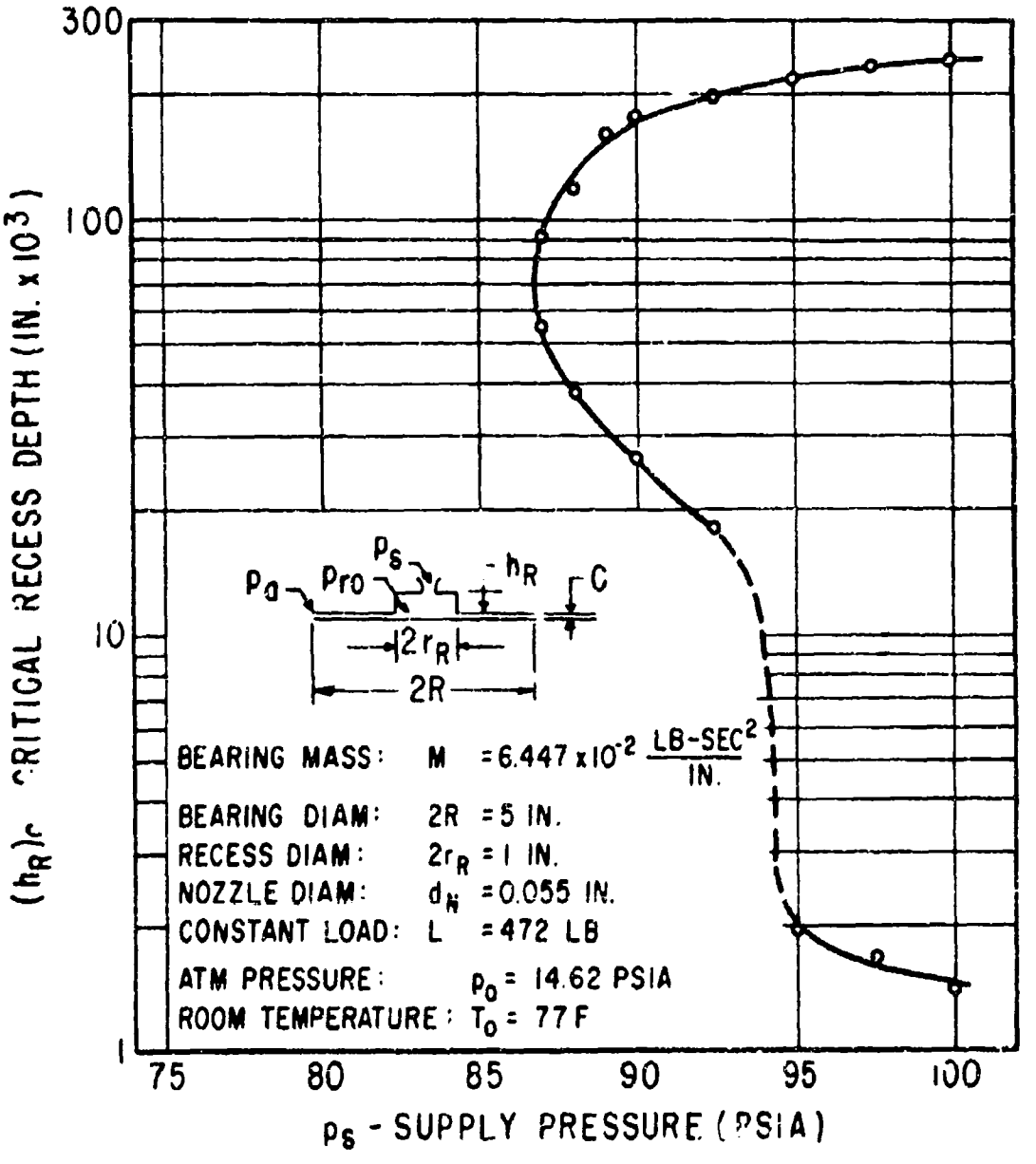

Fig. 9 Experimental Data fr. Licht and Elrod

Unclassified

Security Classification

DOCUMENT CONTROL DATA - R&D

(Security classification of title, body of abstract and indexing annotation must be entered when the overall report is classified)

1. ORIGINATING ACTIVITY (Corporate author) Mechanical Technology Incorporated 968 Albany-Shaker Road Latham, N.Y. 12110	2a. REPORT SECURITY CLASSIFICATION None 2b. GROUP None

3. REPORT TITLE

Analysis of Pneumatic Hammer Instability of Inherently Compensated Hydrostatic Thrust Gas Bearings

4. DESCRIPTIVE NOTES (Type of report and inclusive dates)

Interim (Jan. 1966 - Dec., 1966)

5. AUTHOR(S) (Last name, first name, initial)

Chiang, T., Pan, C.H.T.

6. REPORT DATE	7a. TOTAL NO. OF PAGES	7b. NO. OF REFS
Jan., 1967	43	9

8a. CONTRACT OR GRANT NO.	9a. ORIGINATOR'S REPORT NUMBER(S)
Nonr-3730(00) b. PROJECT NO. NR062-317/4-7-66 c. d.	MTI-66TR47 9b. OTHER REPORT NO(S) (Any other numbers that may be assigned this report)

10. AVAILABILITY/LIMITATION NOTICES

Qualified requestors may obtain copies of this report from DDC

11. SUPPLEMENTARY NOTES	12. SPONSORING MILITARY ACTIVITY
	Office of Naval Research

13. ABSTRACT

Pneumatic hammer instability of an inherently compensated thrust gas bearing was analyzed theoretically. Vohr's experimental correlation between pressure loss coefficient and Reynolds' number was used to calculate flow through the restrictor instead of using the nozzle equations. The time dependent Reynolds' equation was solved by a perturbation analysis for small axial oscillation. Based on the perturbation analysis, dynamic stiffness and damping coefficient were calculated. Utilizing these and Pan's stability criteria (Ref. 6) stability maps were constructed.

DD FORM 1 JAN 64 1473

Unclassified

Security Classification